Low-Grade Hypothalamic Inflammation Leads to Defective Thermogenesis, Insulin Resistance, and Impaired Insulin Secretion

Ana Paula Arruda, Marciane Milanski, Andressa Coope, Adriana S. Torsoni, Eduardo Ropelle, Denise P. Carvalho, Jose B. Carvalheira, and Licio A. Velloso

Laboratory of Cell Signaling (A.P.A., M.M., A.C., A.S.T., L.A.V.), and Department of Internal Medicine (E.R., J.B.C.), University of Campinas, Campinas, Brazil; and Department of Endocrinology (D.P.C.), Federal University of Rio de Janeiro, Rio de Janeiro, Brazil

Hypothalamic inflammation is present in animal models of obesity, and the intracerebroventricular injection of TNFα can reproduce a number of features of the hypothalamus of obese animals. Because obesity is a risk factor for type 2 diabetes (DM2) we hypothesized that, by inducing hypothalamic inflammation, we could reproduce some clinical features of DM2. Lean Wistar rats and TNF receptor 1-knockout mice were employed to determine the effects of hypothalamic actions of TNFα on thermogenesis and metabolic parameters. Signal transduction and protein expression were evaluated by immunoblot and real-time PCR. Thermogenesis was evaluated in living rats, and respirometry was determined in isolated muscle fiber. In Wistar rats, hypothalamic TNFα blunts the anorexigenic effect of leptin, which is accompanied by reduced leptin signaling and increased expression of suppressor of cytokine signaling 3. In addition, hypothalamic TNFα reduces O_2 consumption and the expression of thermogenic proteins in brown adipose tissue and skeletal muscle. Furthermore, hypothalamic inflammation increases base-line plasma insulin and insulin secretion by isolated pancreatic islets, which is accompanied by an impaired insulin signal transduction in liver and skeletal muscle. Hypothalamic inflammation induced by stearic acid also reduces O_2 consumption and blunts peripheral insulin signal transduction. The use of intracerebroventricular infliximab restores O_2 consumption in obese rats, whereas TNF receptor 1-knockout mice are protected from diet-induced reduced thermogenesis and defective insulin signal transduction. Thus, low-grade inflammation of the hypothalamus is sufficient to induce changes in a number of parameters commonly impaired in obesity and DM2, and TNFα is an important mediator of this process. **(*Endocrinology* 152: 1314–1326, 2011)**

Obesity is the main risk factor for type 2 diabetes mellitus (DM2). Over the years, a number of distinct mechanisms have been proposed to explain the common epidemiological association between these conditions. Currently, it is widely accepted that insulin resistance evolves as an outcome of an inflammatory signaling in insulin-sensitive tissues, which is induced by cytokines and other factors produced by the hypertrophied adipose tissue (1, 2). However, recent studies have shown that hypothalamic inflammation and resistance to the adipostatic hormones, leptin and insulin, are early events in the installation of obesity, preceding hypertrophy and insulin resistance in the adipose tissue (3–5). Moreover, targeting inflammation in the hypothalamus by the inactivation of IκB kinase protects against obesity and glucose intolerance (6), suggesting that hypothalamic dysfunction plays an important, and perhaps mechanistic, role in obesity-associated glucose intolerance.

Because the inhibition of hypothalamic inflammation leads to a reduction in body mass (6), it remains unknown

ISSN Print 0013-7227 ISSN Online 1945-7170
Printed in U.S.A.

doi: 10.1210/en.2010-0659 Received June 11, 2010. Accepted December 22, 2010.
First Published Online January 25, 2011

Abbreviations: BAT, Brown adipose tissue; DIO, diet-induced obesity; Dio2, D2 deiodinase; DM2, type 2 diabetes mellitus; HF diet, high-fat diet; icv, intracerebroventricular; IRS1, insulin receptor substrate 1; JAK, Janus family of tyrosine kinases; KO, knockout; PGC1, peroxisomal proliferator-activated receptor-γ coactivator 1; POMC, proopiomelanocortin; SOCS, suppressor of cytokine signaling; STAT, signal transducer and activator of transcription; TNFR1, TNF receptor 1; UCP1, uncoupling protein 1.

whether low-grade hypothalamic inflammation can, *per se*, and independently of body mass change, impair insulin action and other peripheral metabolic parameters that are common to obesity and DM2. We herein demonstrate that a low dose of intracerebroventricular (icv) TNFα is able to mimic some of the features of low-grade/obesity-like hypothalamic inflammation, inducing a broad phenotypic change in the animal and reproducing a number of metabolic features observed in DM2.

Materials and Methods

Antibodies and chemicals

Antibodies against uncoupling protein 1 (UCP1) (goat polyclonal, catalog no. sc-6529), phospho-Janus family of tyrosine kinases (JAK)2 (pJAK2, rabbit polyclonal, catalog no. sc-16566R), suppressor of cytokine signaling (SOCS)3 (rabbit polyclonal, catalog no. sc-9023), phospho-signal transducer and activator of transcription (STAT)3 (pSTAT3, rabbit polyclonal, catalog no. sc-7993) and TNFα (goat polyclonal, catalog no. sc-1347; and rabbit polyclonal, catalog no. sc-8301) were from Santa Cruz Biotechnology (Santa Cruz, CA). Antibody against phospho-FOXO1 (pFOXO1, mouse monoclonal, catalog no. 9461) was from Cell Signaling Technology (Beverly, MA). Antibody against cytochrome C (mouse monoclonal, catalog no. 7H8.2C12) was from BD Biosciences (San Jose, CA). Antibody against β-actin (rabbit polyclonal, ab8227) was from Abcam (Cambridge, MA). Antibody against SERCA 1 (mouse monoclonal, IIH11) was from Affinity BioReagents (Rockford, IL). Rat recombinant TNFα and leptin were from Calbiochem (Cincinnati, OH). All reagents for SDS-PAGE and immunoblotting were from Bio-Rad Laboratories, Inc. (Hercules, CA). HEPES, phenylmethylsulfonyl fluoride, aprotinin, dithiothreitol, Triton X-100, Tween 20, glycerol, BSA fatty acid free (catalog no. A-6003), stearic acid/C18:0 (catalog no. 5376), BSA (fraction V), and angiotensin II were from Sigma-Aldrich (St. Louis, MO). Sodium thiopental, ketamine, and diazepam were from Cristalia (Itapira, Brazil). All the chemicals and primers used in real-time PCR were from Applied Biosystems (Carlsbad, CA). Infliximab was from Centocor (Horsham, PA).

Animal models

Experiments were performed with male Wistar rats (250–300 g), male Zucker rats (fa/fa, 400–450 g), male TNFRp55−/− mice [TNF receptor (TNFR)1-knockout (KO)], and its respective control, C57BL/6J. Wistar and Zucker rats were obtained from the University of Campinas Animal Breeding Center. Mice were originally from The Jackson Laboratory (West Grove, PA) and kindly donated by Dr. J. S. Silva from the University of São Paulo (7). All experimental animals were maintained in individual cages with water and diet *ad libitum* and on a 12-h light, 12-h dark cycle. The mice were bred under specific pathogen-free conditions. All experiments were conducted in accordance with the principles and procedures described by the National Institutes of Health Guidelines for the Care and Use of Experimental Animals and were approved by the University of Campinas Ethical Committee.

Intracerebroventricular cannulation

Wistar rats were stereotaxically instrumented using a Stoelting stereotaxic apparatus, according to a previously described method (8). Cannula efficiency was tested 1 wk after cannulation by the evaluation of the drinking response elicited by icv angiotensin II (9). Stereotaxic coordinates were: anteroposterior, 0.2 mm/lateral, 1.5 mm/depth, 4.0 mm. In some experiments we used the coordinates anteroposterior, −1.8 mm/lateral, 1.0 mm/depth, 4.0 mm; or, anteroposterior, −1.8 mm/lateral, 1.0 mm/depth, 2.0 mm to place the cannula in the hippocampus or in the upper portion of the midbrain, respectively. icv-cannulated rats were treated for 4 or 8 d, once a day, with TNFα (2.0 μl, 10^{-12} to 10^{-8} M). The TNFα doses used in this study were based on previous studies (4, 8). In some experiments, icv cannulated rats were treated for 4 d, once a day, with stearic acid (45, 90, or 180 μg in 2.0 μl). Stearic acid was diluted in ultrapure water containing hydro-biodegradable plastic detergent (0.1%) and fatty acid free BSA (75 mM). For the experiment with infliximab, 8-wk-old male Wistar rats were fed on a high-fat (HF) diet containing 36 g% fat from animal source for 8 wk. The macronutrient composition of the diet was presented elsewhere (10). Subsequently, the animals were divided into two groups, paired by body mass, and treated icv with saline (2 μl once a day) or infliximab (0.2 μg in 2 μl) once a day for 7 or 8 d (11).

Tumor xenograft model

The Walker-256 tumor cell line (originally obtained from the Christ Hospital Line, National Cancer Institute Bank, Cambridge, UK) is currently maintained frozen in liquid nitrogen. Walker-256 tumor cells were obtained from the ascitic fluid of the peritoneal cavity of Wistar rats, 5 d after the ip injection of 20×10^6 cells. After cell harvesting, the percentage of viable cells was determined using 1% Trypan blue solution in a Neubauer chamber. Tumor cells (2×10^6 cells in 1 ml saline solution) were injected in the right flank of rats weighing 250–300 g. Each animal's individual baseline 24-h food intake was defined as the average daily food intake over a period of three consecutive days. In tumor-bearing animals, cancer anorexia was defined as a single value of less than 70% baseline, occurring after a steady decline of at least 3 d duration. When criteria for anorexia had been met, tumor-bearing animals were used in experimental protocols for determination of TNFα expression in the hypothalamus and evaluation of spontaneous food intake (11, 12).

Experimental protocols employed with the TNFR1-KO mice

Male TNFR1-KO mice (8 wk of age) and their controls (C57BL/6) were divided into two groups paired by body mass and assigned to receive two distinct diets for 8 wk: a standard rodent chow (SC) or a HF diet. Experiments were performed at the end of the 8-wk period.

Protocol for food ingestion determination

For the leptin sensitivity test, icv cannulated rats were food deprived for 6 h (from 12–18 h) and, at 18 h, were icv treated with saline (2 μl), leptin (2 μl, 10^{-6} M), TNFα (2 μl, 10^{-8} to 10^{-12} M), or with combinations of TNFα and leptin. Food ingestion was determined over the next 12 h (8). This dose provide local concentrations of leptin that were similar to physiological post-meal levels (550–1000 pM) (13).

Immunoblotting

For evaluation of protein expression in the hypothalami, brown adipose tissue (BAT), liver, and soleus muscle, the specimens were excised and immediately homogenized in solubilization buffer [1% Triton X-100, 100 mM Tris-HCl (pH 7.4), 100 mM sodium pyrophosphate, 100 mM sodium fluoride, 10 mM EDTA, 10 mM sodium orthovanadate, 2.0 mM phenylmethylsulfonylfluoride and 0.1 mg aprotinin/ml] at 4 C with a Polytron PTA 20S generator (model PT 10/35; Brinkmann Instruments, Westbury, NY). Insoluble material was removed by centrifugation for 15 min at 9000 × *g*. The protein concentration of the supernatants was determined by the Bradford dye-binding method. In immunoblot experiments, 0.05–0.2 mg of protein extracts was separated by SDS-PAGE, transferred to nitrocellulose membranes, and blotted with specific antibodies, as described in the figure legends. Specific bands were detected by chemiluminescence, and visualization/capture was performed by exposure of the membranes to RX-films. For experiments that measured insulin signaling, the abdominal cavities of anesthetized mice were opened, and the animals received an injection of insulin (100 μl, 10^{-6} M) or saline (100 μl) through the cava vein. After different intervals (2 or 15 min for insulin receptor substrate 1 (IRS1) and FOXO1, respectively), fragments (3.0 × 3.0 × 3.0 mm) of soleus muscle and liver were excised and immediately homogenized in the same solubilization buffer described above and blotted with IRS1, FOXO1, or pFOXO1 antibodies. For determination of tyrosine phosphorylation of IRS1, 0.5 mg total protein was submitted to immunoprecipitation with anti-IRS1 antibody. Immunocomplexes were resolved by SDS-PAGE, transferred to nitrocellulose membranes, and immunoblotted with antiphosphotyrosine antibody (14).

Real-time PCR

The expressions of UCP1, peroxisomal proliferator-activated receptor-γ coactivator 1 (PGC1)α, D2 deiodinase (Dio2), neuropeptide Y, Agouti-related peptide, TRH, CRH, proopiomelanocortin (POMC), melanin-concentrating hormone; cocaine and amphetamine-regulated transcript, and IL-1β mRNAs were measured in samples (BAT, soleus muscle, or hypothalamus) obtained from rats treated icv with saline (control) or TNFα 10^{-12} M or in rats fed on HF diet and treated or not with infliximab icv. UCP1 was also determined in the BAT of control and TNFR1-KO mice fed on chow or HF diet. Intron-skipping primers were obtained from Applied Biosystems (Foster City, CA). Glyceraldehyde-3-phosphate dehydrogenase primers were used as a control. Real-time PCR analysis of gene expression was performed in an ABI Prism 7700 sequence detection system (Applied Biosystems). The optimal concentration of cDNA and primers, as well as the maximum efficiency of amplification, was obtained through five-point, 2-fold dilution curve analysis for each gene. Each PCR contained 3.0 ng of reverse-transcribed RNA, 200 nM of each specific primer, TaqMan (Applied Biosystems), and ribonuclease free water to a final volume of 20 μl. Real-time data were analyzed using the Sequence Detector System 1.7 (Applied Biosystems) (15).

Indirect calorimetry and body temperature

O_2 consumption, CO_2 release, and respiratory exchange ratio (RER) were measured in fed animals through an indirect open-circuit calorimeter (Oxymax Deluxe System; Columbus Instruments, Columbus, OH), as described previously (4). Rectal temperature was measured with a digital thermometer, and the values presented represent the mean of the temperatures at the end of the experimental period.

Skeletal muscle oxygen consumption and citrate synthase activity

Fragments (1–3 mg) of the soleus muscle were placed in a Petri dish on ice with 1 ml of relaxing solution containing 10 mM Ca^{2+}/EGTA buffer,0.1 μM free calcium, 20 mM imidazole, 50 mM K^+/4-morpholinoethanesulfonic acid, 0.5 mM dithiothreitol, 6.56 mM $MgCl_2$, 5.77 mM ATP, 15 mM phosphocreatine (pH 7.1), and individual fiber bundles were separated with sharp forceps. The fiber bundles were permeabilized for 30 min in an ice-cold relaxing solution containing saponin (50 μg/ml). The fibers were washed twice for 10 min each. The muscle bundles were then immediately transferred into an OROBOROS respirometer (Innsbruck, Austria) containing an air-saturated respiration medium at 37 C. Oxygen consumption was measured in the respiration medium, MiR05, containing 60 mM potassium lactobionate, 0.5 mM EGTA, 3 mM $MgCl_2.6H_2O$, 20 mM taurine, 10 mM KH_2PO_4, 20 mM HEPES, 110 mM sucrose, 2 mg/ml BSA (pH 7.1), in the presence of 7 mM pyruvate and 4 mM malate. The respiration rate in state III was measured after addition of ADP (2 mM) and that of state IV was measured in the presence of oligomycin (1 μg/ml). The Oxygraph-2k is a two-chamber titration-injection respirometer with a limit of oxygen flux detection of 1 pmol/sec · ml. Citrate synthase activity was determined spectophotometrically, as described previously (7).

ELISA for TNFα determination

Tissue TNFα levels were determined in samples of hypothalamic protein extracts (2.0 mg/ml). Serum samples obtained from control and icv treated rats were also used for determination of TNFα. Both serum and tissue TNFα were measured by ELISA (Pierce Biotechnology, Rockford, IL), following the recommendations of the manufacturer.

Hormone determinations

Insulin was determined by RIA as previously described (16). T3 and T4 in serum were determined by RIA commercial method (Cout-a-count; Siemens, Berlin, Germany). The insulin intraassay coefficient of variability is 5.1–7.6%; the T3 intraassay coefficient of variability is 6.1–8.9%; and the T4 intraassay coefficient of variability is 2.7–3.8%.

Insulin secretion studies

Islets were isolated by hand picking following collagenase digestion (17). To measure insulin secretion, groups of five islets were preincubated for 45 min at 37 C in Krebs-bicarbonate buffer. The solution was then replaced by fresh buffer containing low (2.8 mmol/liter) or supraphysiological (16.7 mmol/liter) concentrations of glucose, and the islets were incubated for 1.0 h. The insulin content of the medium at the end of the incubation period was determined by RIA.

Statistical analysis

Mean values ± SEM obtained from densitometry scans, real-time PCR, body mass determination, food intake, and hormone levels were compared using Tukey-Kramer test (ANOVA) or

Student's *t* test, as appropriate; $P < 0.05$ was accepted as statistically significant.

Results

Effects of different concentrations of TNFα in the hypothalamus

Previous studies have shown that TNFα expression is increased in the hypothalamus of animal models of obesity. However, it has been suggested that, depending on its local concentrations, TNFα can exert a dual function in the hypothalamus, being catabolic at high concentration and anabolic at low concentration, and thus, inhibiting the actions of leptin and insulin (18). Using an ELISA we show that TNFα levels in the hypothalamus are increased in both genetic and diet-induced obesity (DIO), as well as in cancer (Fig. 1A). However, the concentration of TNFα in the hypothalamus of tumor-bearing animals is significantly higher than in either model of obesity and is accompanied by a significantly lower spontaneous food consumption (Fig. 1B). The icv injection of high doses of TNFα (2.0 μl, 10^{-8} to 10^{-11}M) reproduce some features of cancer-induced cachexia, such as reduced food intake, loss of body mass, increased body temperature, and increased oxygen consumption (Fig. 1, C–G). Conversely, the icv injection of a low-dose of TNFα (2.0 μl, 10^{-12} M) is devoid of a catabolic outcome and, in fact, exerts an anabolic action, reducing oxygen consumption and carbon dioxide production (Fig. 1, C–G). Neither high-, nor low-dose icv TNFα leads to changes in blood levels of this cytokine (data not shown).

Low-dose hypothalamic TNFα inhibits leptin action and reduces the expression of thermogenic neurotransmitters

The icv hypothalamic treatment with a low dose of TNFα inhibits the anorexigenic effect of leptin (Fig. 2A), which is accompanied by reduced leptin signal transduction through JAK2 (Fig. 2B) and STAT3 (Fig. 2C) and increased expression of the inhibitory protein, SOCS3 (Fig. 2D). Low-dose TNFα alone for 4 d exerted no significant effect on food intake (Fig. 1C) and body mass variation (Fig. 1D); however, extending the icv hypothalamic treatment with a low-dose TNFα for 8 d leads to a significant increase in body mass gain (Fig. 2E). The effect of TNFα in the hypothalamus was specific because the treatment with a low-dose TNFα, icv injected in the hippocampus or in the upper portion of the midbrain, exerted no effect on food intake or body mass (data not shown). Because leptin is one of the main modulators of hypothalamic neurotransmitter expression, we measured mRNA levels of the most relevant neurotransmitters of the hypothalamus involved in the control of feeding and thermogenesis. As depicted in Fig. 2F, TNFα negatively affects the expressions of POMC, TRH, and CRH, three neurotransmitters with important thermogenic function.

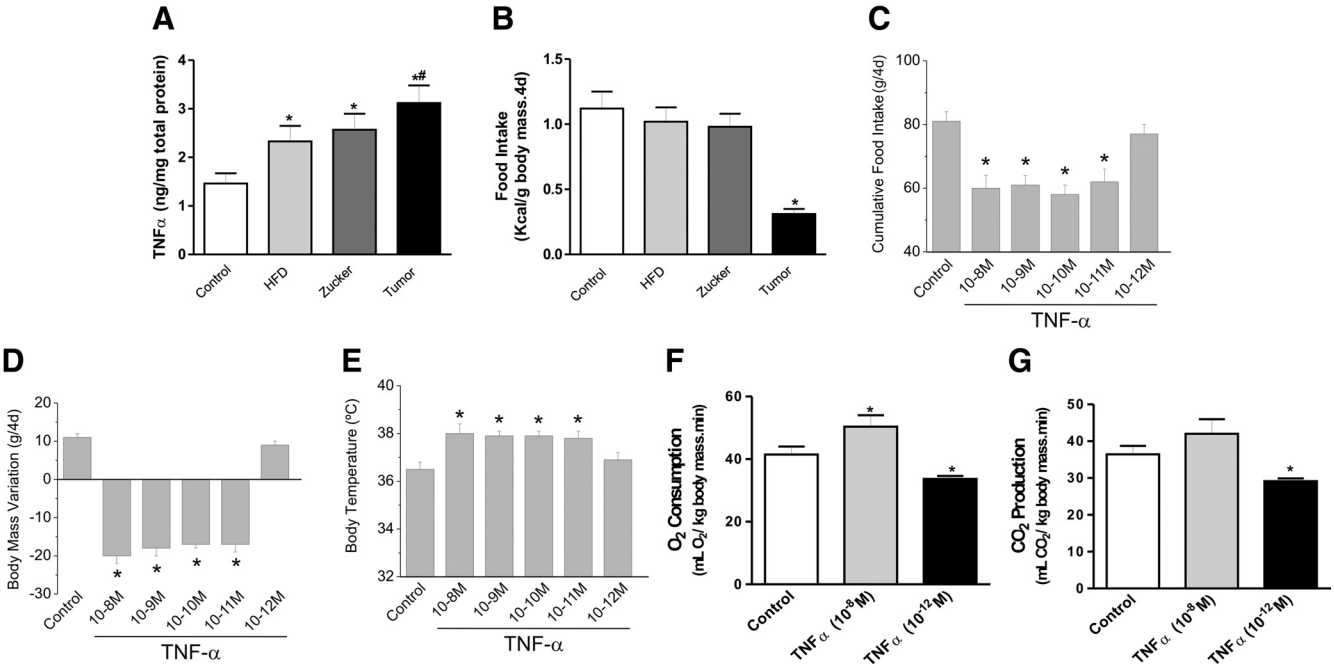

FIG. 1. Differential effects of low- and high-hypothalamic TNFα levels on whole-body metabolism. TNFα protein level was determined by ELISA in whole-protein extracts obtained from the hypothalami of lean (Control), diet-induced obese [high-fat diet (HFD)], genetically determined obese (Zucker), and tumor-bearing rats (A). Relative food intake in 4 d was determined in the same groups (B). Cumulative food intake (C), body mass variation (D), and body temperature (E) were determined in rats treated icv with saline (Control), or 2 μl 10^{-8} to 10^{-12} M TNFα icv for 4 d. O_2 consumption (F) and CO_2 production (G) in respirometric assay were determined in Wistar rats treated icv with saline (Control), 2 μl 10^{-8}, or 10^{-12} M TNFα icv for 4 d. In all experiments, n = 5; *, $P < 0.05$ *vs.* Control; in panel A, #, $P < 0.05$ *vs.* HFD.

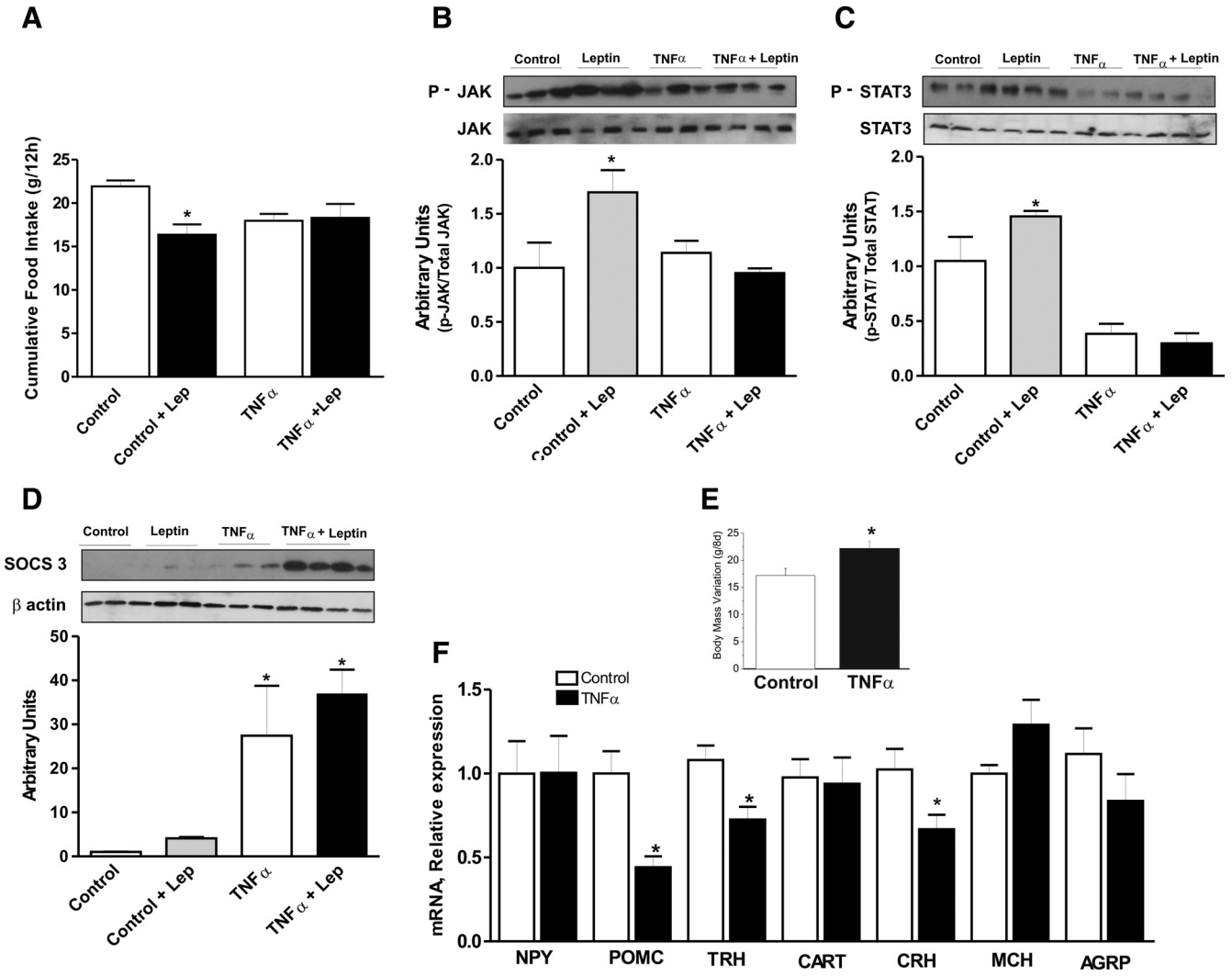

FIG. 2. Effect of low-dose hypothalamic TNFα on leptin action and neurotransmitter expression. Wistar rats were icv treated with saline (Control) or TNFα (2 μl, 10^{-12} M) for 4 d and then chased with saline or leptin (Lep) (2 μl, 10^{-6} M) icv. Spontaneous food intake (A) was determined over 12 h. Signal transduction through JAK2 (phospho-JAK2, P-JAK) (B) and STAT3 (phospho-STAT3, P-STAT3) (C), and the expression of SOCS3 (D) were evaluated by immunoblot. Lean rats were icv treated with saline (control) or TNFα (2 μl, 10^{-12} M) for 8 d, and body mass variation was determined (E). The expressions of hypothalamic neurotransmitters were determined by real-time PCR in samples from rats treated icv with saline (control) or TNFα (2 μl, 10^{-12} M) for 4 d (F). In all experiments, n = 5; in panels A–C and E–F, *, $P < 0.05$ *vs.* Control; in panel D, *, $P < 0.05$ *vs.* control and *vs.* control + leptin. CART, Cocaine and amphetamine-related transcript; MCH, melanin-concentrating hormone; NPY, neuropeptide Y.

Low-dose hypothalamic TNFα inhibits thermogenesis

BAT and skeletal muscle are the effectors of most of the thermogenic activity in rodents (19, 20). The icv injection of low-dose TNFα produces significant reductions in the expressions of UCP1, cytochrome *c*, PGC-1α, and Dio2 in BAT (Fig. 3, A–C). In addition, hypothalamic TNFα reduces mitochondria respiration in isolated muscle fibers (Fig. 3D), which is accompanied by reduced cytochrome *c* expression (Fig. 3E) and citrate synthase activity (Fig. 3F), but no alteration in SERCA1 expression was detected (Fig. 3E). Moreover, hypothalamic TNFα exerts no effect on the blood levels of the thyroid hormones T3 (Fig. 3G) and T4 (Fig. 3H).

Low-dose hypothalamic TNFα affects insulin secretion and action

To evaluate the systemic outcomes of a low-grade hypothalamic inflammation, rats were icv treated with a low-dose of TNFα, and insulin secretion and action in peripheral tissues were determined. The blood level of insulin (Fig. 4A), as well as the baseline secretion of insulin by isolated pancreatic islets (Fig. 4B), are significantly increased in TNFα-treated rats. However, upon glucose stimulation the ratio insulin secretion in 16.7 mM glucose/insulin secretion in 2.8 mM glucose in TNFα-treated rats is only 65% of controls (Fig. 4C). Moreover, upon hypothalamic TNFα treatment, insulin signal transduction through IRS1 and FOXO1 is significantly impaired in liver (Fig. 4, D and E) and skeletal muscle (Fig. 4, F and G) of rats.

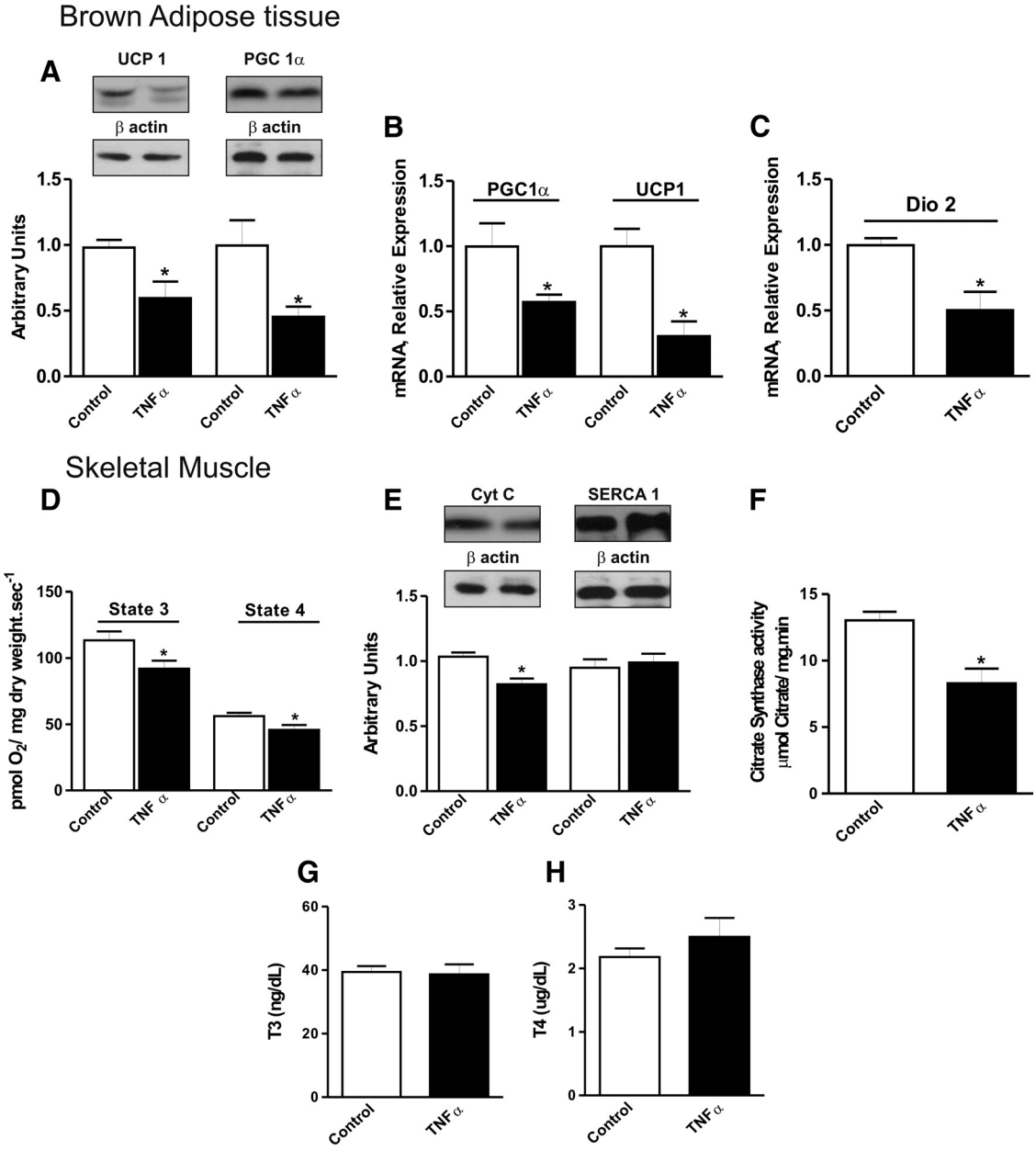

FIG. 3. Effect of low-dose hypothalamic TNFα on thermogenesis. UCP1, PGC1α, and Dio2 were determined in BAT of rats treated for 4 d icv with saline (Control) or TNFα (2 μl, 10^{-12} M). UCP1 and PGC1α were measured by immunoblot (A) and real-time PCR (B), whereas Dio2 was measured only by real-time PCR (C). O_2 consumption was evaluated by an isolated skeletal muscle fiber respirometric assay (D). The expression of cytochrome c (Cyt C) and SERCA1 was measured by immunoblot (E). Citrate synthase activity in skeletal muscle was measured by spectrophotometry (F). Serum levels of T3 (G) and T4 (H) were measured by RIA. In all experiments, n = 5; *, $P < 0.05$ *vs.* Control.

Saturated fatty acid-induced inflammation of the hypothalamus reproduces the effects of low-dose hypothalamic TNFα

Saturated fatty acids induce hypothalamic inflammation through the activation of TLR4 signaling and endoplasmic reticulum stress (4, 21). The icv injection of stearic acid (C18:0) produces a dose-dependent increase of TNFα in the hypothalamus (Fig. 5A), which is accompanied by reduced oxygen consumption (Fig. 5B), reduced carbon dioxide production (Fig. 5C), and reduced expression of UCP1 in BAT (Fig. 5I). In addition, icv stearic acid impairs insulin signal transduction through IRS1 and FOXO1 in liver (Fig. 5, D and E) and IRS1 in skeletal muscle (Fig. 5, F and G). The icv treatment with the anti-TNFα monoclonal antibody infliximab, reduces stearic acid-induced IL1β expression in the hypothalamus (Fig. 5H) and restores the levels of UCP1 in BAT (Fig. 5I) without affecting the expression of cytochrome *c* in BAT (Fig. 5J).

Reversal of the antithermogenic effects of DIO with icv infliximab

The systemic use of the anti-TNFα monoclonal antibody, infliximab, improves insulin signal transduction in periph-

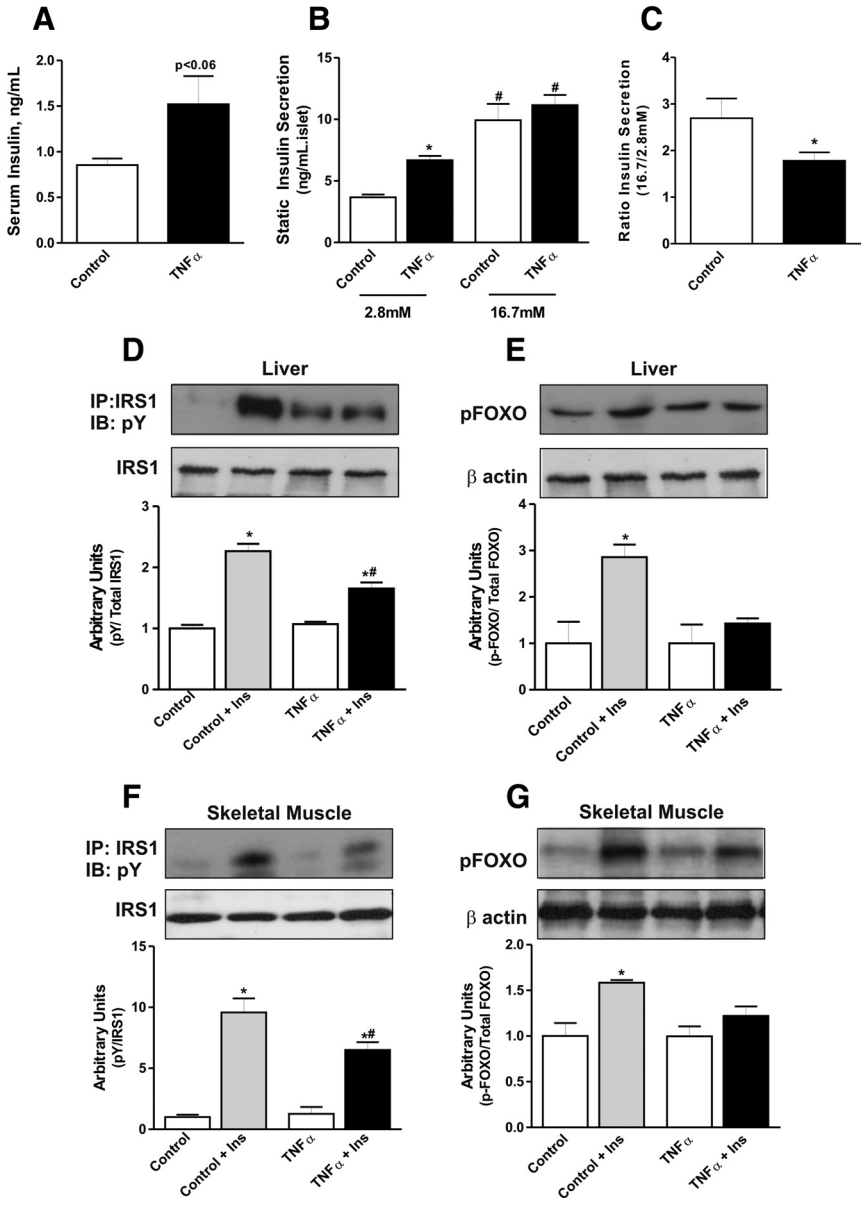

FIG. 4. Effect of low-dose hypothalamic TNFα on insulin secretion and action. In panels A–C, Wistar rats were icv treated with saline (Control) or TNFα (2 μl, 10^{-12} M) for 4 d. Serum insulin levels were determined by RIA (A). Insulin secretion by isolated pancreatic islets was evaluated in islets exposed to 2.8 and 16.7 mM glucose and measured by RIA (B). An index of pancreatic islet responsiveness to glucose was obtained by the ratio of secretion in 16.7/2.8 mM (C). In panels D–G, Wistar rats were icv treated with saline (Control) or TNFα (2 μl, 10^{-12} M) for 4 d. The rats were then anesthetized and submitted to a venous (cava vein) injection of saline or insulin (Ins) (100 μl, 10^{-6} M). Samples of liver (D and E) and skeletal muscle (F and G) were employed for the determination of insulin-induced tyrosine phosphorylation of IRS1 (D and F) and serine phosphorylation of FOXO1 (p-FOXO) (E and G). IRS1 tyrosine phosphorylation was evaluated in total protein extracts submitted to immunoprecipitation (IP) with anti-IRS1 antibodies and immunoblot (IB) with anti-phosphotyrosine (pY) antibodies. In all experiments, n = 5; *, $P < 0.05$ *vs.* Control; in panel B, #, $P < 0.05$ *vs.* Control and TNFα 2.8 mM; in D and F, #, $P < 0.05$ *vs.* TNFα.

eral tissues of diet-induced obese mice (14). To determine the impact of TNFα and low-grade hypothalamic inflammation in systemic metabolic parameters, DIO rats were icv treated with infliximab, and markers of thermogenesis and insulin signal transduction were evaluated. Figure 6, A and B, shows that infliximab corrects the defective oxygen consumption/carbon dioxide production of DIO rats. In addition, the expression of UCP1 in BAT is increased to levels similar to those of lean controls (Fig. 6C). Interestingly, hypothalamic infliximab is also effective for improving insulin signal transduction through IRS1 in the liver (Fig. 6D) and muscle (Fig. 6E), which is accompanied by improved whole-body insulin action, as determined by an insulin tolerance test (Fig. 6F), whereas no changes in insulin secretion are detected (data not shown). Upon prolonged infliximab icv treatment (8 d), a significant reduction of body mass gain is achieved (Fig. 6G), with no significant change of food intake (data not shown).

TNFR1-KO mice present increased thermogenesis and improved insulin signal transduction in peripheral tissues

To explore the role of the main TNFα receptor type, TNFR1, in DIO-dependent defects in thermogenesis and insulin signaling, TNFR1-KO mice were submitted to a HF diet, and parameters of thermogenesis and insulin signal transduction were studied. As depicted in Fig. 7, A and B, KO mice are protected from DIO even consuming a similar amount of calories as control. Chow-fed KO mice consume more oxygen than controls and, when fed on a HF diet, this is significantly increased (Fig. 7C). No differences in CO_2 production and in blood T3 and T4 levels are detected among the groups (Fig. 7, D–F). However, UCP1 expression in BAT is significantly increased in KO mice (Fig. 7G). This is accompanied by improved insulin signal transduction through IRS1 and FOXO1 in liver (Fig. 7, H and I) and muscle (Fig. 7, J and K).

Discussion

Type 2 diabetes mellitus (DM2) results from the complex combination of insulin resistance and defective pancreatic β-cell function (22). Most subjects with DM2 are over-

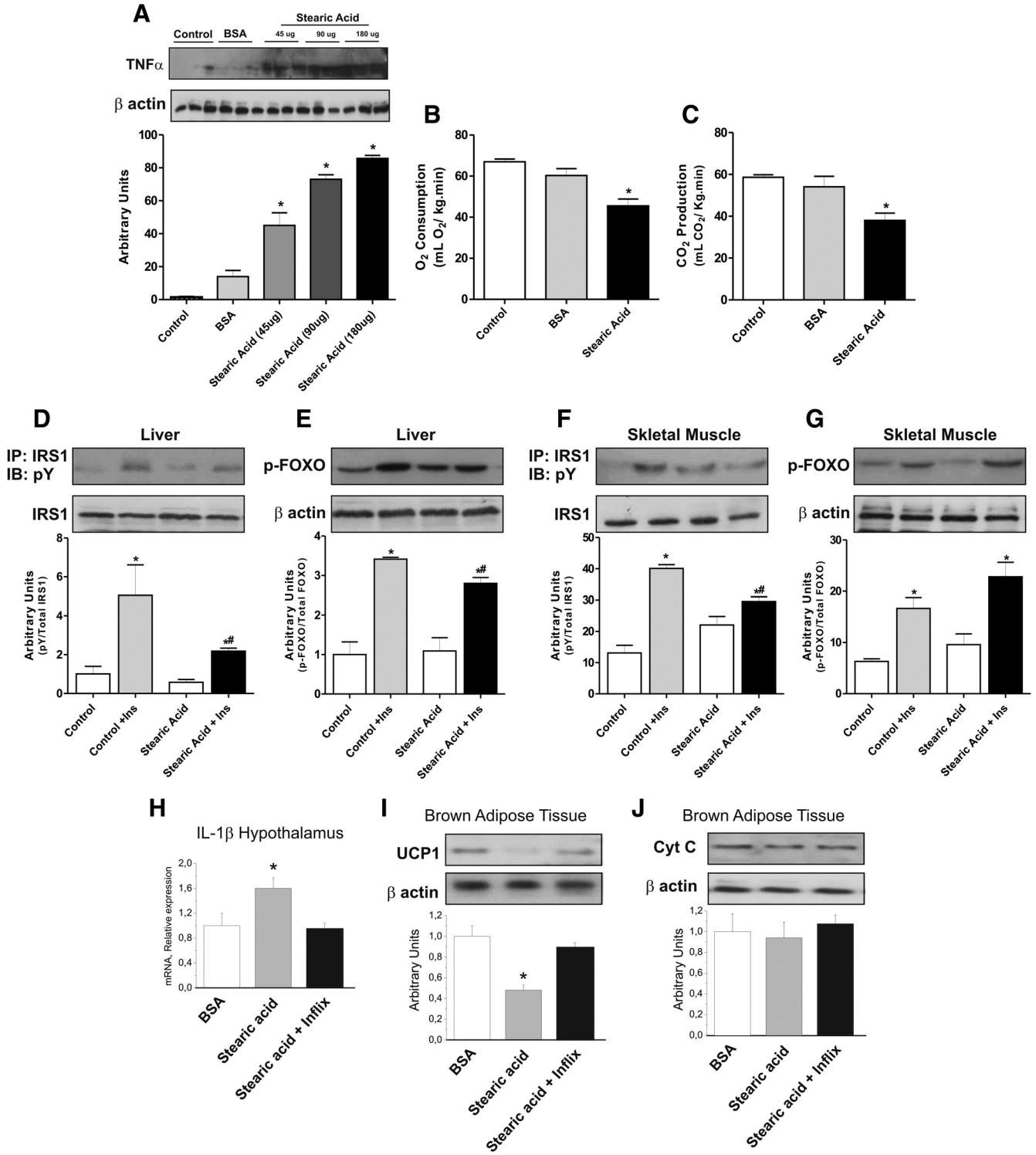

FIG. 5. Effects of stearic acid in the hypothalamus. Wistar rats were treated icv once a day for 4 d, with 2 μl saline (Control), BSA, or stearic acid (containing 90 μg, or the amount depicted in panel A). TNFα protein expression was determined by immunoblot (IB) in total protein extracts from hypothalami (A). O_2 consumption (B) and CO_2 production (C) were determined by respirometry. In panels D–G, rats were injected with a single iv (cava vein) dose of insulin (Ins) (100 μl, 10^{-6} M) and samples from liver (D and E) and skeletal muscle (F and G) were obtained after 2 or 15 min for IRS1 or FOXO1, respectively; in panels D and F, IRS1 tyrosine phosphorylation was evaluated in total protein extracts submitted to immunoprecipitation (IP) with anti-IRS1 antibodies and immunoblot (IB) with anti-phosphotyrosine (pY) antibodies; in panels E and G, serine phosphorylation of FOXO1 (p-FOXO) was evaluated by immunoblot. IL1β mRNA expression was evaluated by real-time PCR in the hypothalamus of icv BSA, stearic acid, or stearic acid + infliximab-treated rats (H). The same rats were employed for evaluations of UCP1 (I) and cytochrome C (Cyt C) (J) protein expressions by immunoblot in total protein extracts from BAT. In all experiments, n = 5; in panels A–G, *, $P < 0.05$ *vs.* Control; in panels H and I, *, $P < 0.05$ *vs.* BSA; in panels D–F, #, $P < 0.05$ *vs.* Control+insulin.

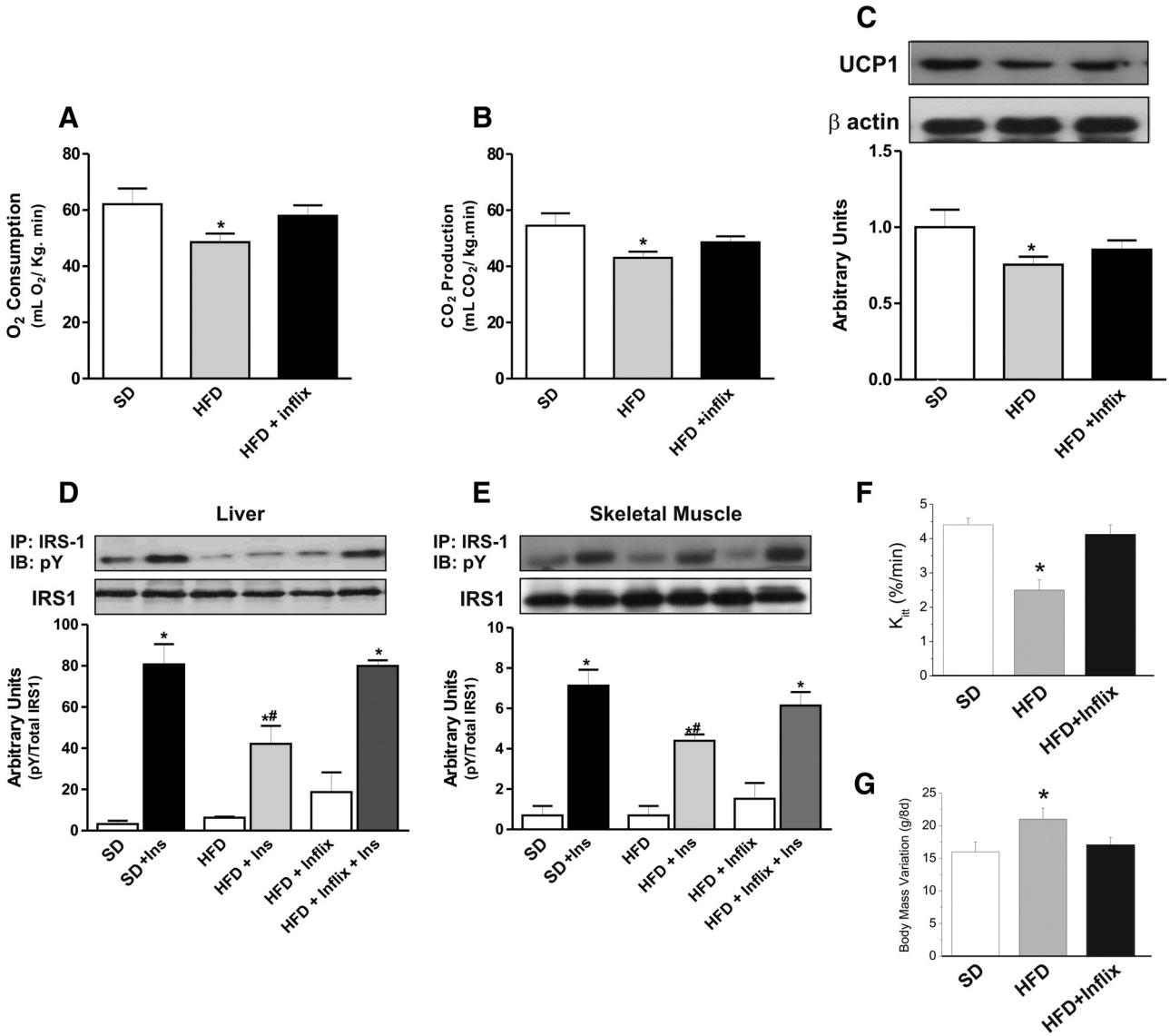

FIG. 6. Effect of inhibition of TNFα on the hypothalamus of obese rats. Lean [standard diet (SD)] or diet-induced obese high-fat diet (HFD) Wistar rats were treated icv with saline or infliximab (0.2 μg in 2 μl) once a day for 7 d and then employed for evaluation of O_2 consumption (A) or CO_2 production by respirometry (B). BAT was obtained for determination of UCP1 expression by immunoblot (C). Some rats were acutely injected with a single intravenous (cava vein) dose of insulin (Ins) (100 μl, 10^{-6} M), and samples from liver (D) and skeletal muscle (E) were obtained after 2 min; IRS1 tyrosine phosphorylation was evaluated in total protein extracts submitted to immunoprecipitation (IP) with anti-IRS1 antibodies and immunoblot (IB) with anti-phosphotyrosine (pY) antibodies. An insulin tolerance test was performed in , SD, HFD, and HFD + infliximab rats; the result is expressed as the constant of glucose decay (Kitt) (F). Body mass variation was evaluated during 8 d in SD, HFD, and HFD + infliximab rats (G). In all experiments, n = 5; in panels A–G, *, $P < 0.05$ *vs.* SD; in panels D and E, #, $P < 0.05$ *vs.* SD+insulin.

weight, and obesity-related factors have been proposed as important determinants of the loss of glucose homeostasis. Inflammatory molecules, produced by the enlarged adipose tissue, activate serine/threonine kinases in insulin-sensitive cells, which impair signal transduction, resulting in insulin resistance (1). As insulin resistance progresses, the pancreatic β-cell increases secretion to compensate for peripheral demand. This compensation may fail depending on the genetic background and on the presence of harmful factors such as inflammatory molecules produced by the adipose tissue and excessive circulating nutrients, such as fatty acids and sugars (22). Behavioral or pharmacological approaches aiming at reducing body mass, restraining insulin resistance, and/or improving β-cell function correct hyperglycemia and are widely used to treat DM2 (23, 24).

After the characterization of inflammation as an important mechanism inducing hypothalamic dysfunction in obesity, it was shown that targeting hypothalamic inflammation by distinct means produced beneficial effects in body mass and also in peripheral insulin action (4, 6, 21). However, it was not clear whether these outcomes resulted only from body mass reduction or were a consequence of improved hypothalamic activity, acting in parallel with body mass change.

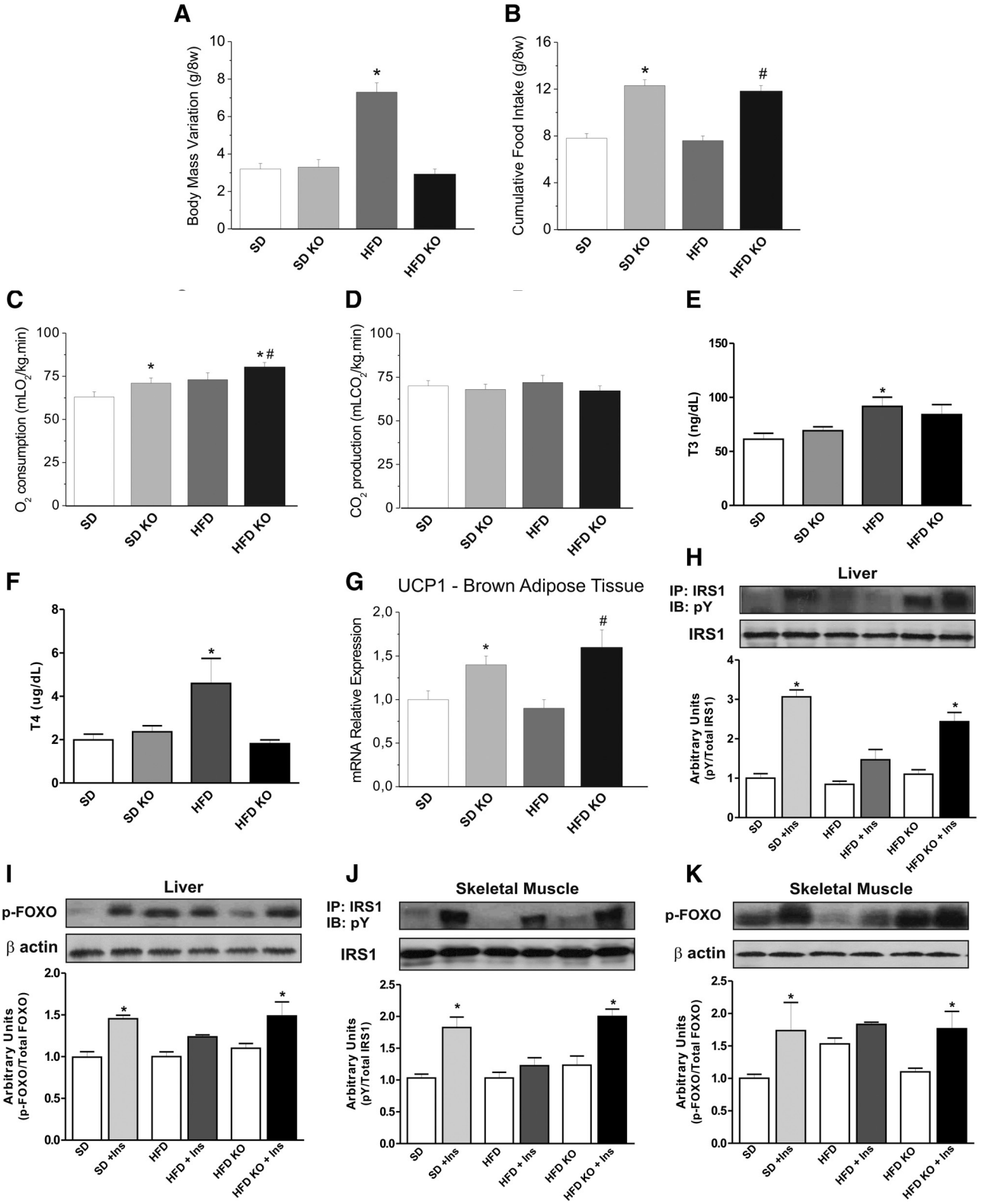

FIG. 7. Outcomes of DIO in TNFR1-KO. Control and TNFR1-KO mice were fed either regular chow [standard diet (SD) and SD KO] or high-fat diet (HFD and HFD KO) for 8 wk and body mass variation (A) and cumulative food intake (B) were determined. O_2 consumption (C) or CO_2 production (D) were evaluated by respirometry. The serum levels of T3 (E) and T4 (F) were measured by RIA. UCP1 mRNA expression in the BAT was evaluated by real-time PCR (G) In panels H–K, mice were injected with a single iv (cava vein) dose of insulin (Ins) (100 μl, 10^{-6} M), and samples from liver (H and I) and skeletal muscle (J and K) were obtained after 2 or 15 min for IRS1 or FOXO1, respectively; in panels H and J, IRS1 tyrosine phosphorylation was evaluated in total protein extracts submitted to immunoprecipitation (IP) with anti-IRS1 antibodies and immunoblot (IB) with anti-phosphotyrosine (pY) antibodies; in I and K, serine phosphorylation of FOXO1 (p-FOXO) was evaluated by immunoblot. In all experiments, n = 5; in panels A–G, *, $P < 0.05$ *vs.* SD and #, $P < 0.05$ *vs.* HDF; in panels H–K, *, $P < 0.05$ *vs.* respective condition without insulin.

TNFα is one of the main inflammatory factors produced by the hypothalamus in response to dietary intervention (3, 4). Both microglia and neurons can express this cytokine, which plays an important role in the induction of hypothalamic resistance to leptin and insulin (3). Interestingly, hypothalamic inflammation may exert a paradoxical effect on energy metabolism. Although at high magnitude, such as in cancer and sepsis, it leads to catabolism, at a low level, as observed in obesity, it has the opposite effect (18). In the first part of this study, we showed that the level of hypothalamic TNFα protein is significantly higher in tumor-bearing, compared with control rats. In obese animals, TNFα levels are also higher than controls but significantly lower than tumor-bearing rats. In both cases, the increased levels of hypothalamic TNFα are accompanied by changes in feeding behavior, which are inhibited in tumor-bearing and increased in obese animals. Moreover, icv injection of a high concentration of TNFα reproduces a number of phenotypic features of cachexia, whereas at a low concentration it is clearly anabolic. It is interesting to notice that the effects of TNFα change sharply when the dose is increased by only 10-fold. This is in pace with the small differences in the levels of TNFα when comparing obesity and cancer, as shown here and elsewhere (25, 26). Thus, it is attractive to propose that the inflammatory paradox of the hypothalamus is a result of a difference in the magnitude of the inflammatory process. In the case of sepsis and cancer, most inflammatory factors are systemic and high, reaching the central nervous system via the bloodstream. In obesity, the systemic levels of inflammatory factors are increased, compared with lean subjects, but are considerably lower than in cachexia. However, in DIO, cytokines are also produced in the hypothalamus (3, 4), and it is not yet known whether low-grade inflammation results only from the action of locally produced cytokines or from the combination of local and systemic inflammatory factors.

When obesity is induced by a Western diet, the hypothalamus is the first tissue to exhibit molecular resistance to insulin (5). This fact, taken together with the results of other studies that show an improvement in peripheral insulin resistance, after the inhibition of hypothalamic inflammation (6, 21), suggest that the diabetes-like phenotype can be induced by hypothalamic dysfunction. To evaluate the isolated effect of low-grade hypothalamic inflammation on peripheral insulin action, lean rats were treated icv with a low dose of TNFα. This treatment produced an impairment of leptin anorexigenic effect and defective leptin signaling through JAK2 and STAT3, accompanied by increased hypothalamic expression of SOCS3. All these outcomes are similar to the findings reported in a number of animal models of obesity (27, 28). In addition, hypothalamic TNFα led to reductions in POMC, TRH, and CRH, all of which are neurotransmitters with important thermogenic functions. This was accompanied by the negative regulation of important players in BAT and skeletal muscle thermogenesis, as seen in animal models and humans with glucose intolerance or diabetes (29).

Next, we evaluated the outcomes of low-grade hypothalamic inflammation on insulin secretion and action. In DM2, both the action and secretion of insulin become defective, and it is believed that hyperglycemia will develop only when both these functions emerge together (22, 30). A short-term treatment with low-dose TNFα in the hypothalamus had no effect on glucose levels (data not shown). However, hyperinsulinemia was evident, and defective insulin secretion by isolated pancreatic islets reproduced features commonly seen in diabetic subjects and experimental animals (31, 32). Moreover, the evaluation of insulin signal transduction in liver and muscle revealed a reduced insulin-induced activation of IRS1 and FOXO1, which is a molecular hallmark of insulin resistance seen in distinct animal models and humans with glucose intolerance or diabetes (32).

In DIO, saturated fatty acids induce inflammatory signal transduction in the hypothalamus by at least two distinct mechanisms: 1) activation of TLR4 (4), and; 2) activation of PKCτ (33). When rats were treated with stearic acid icv, the expression of TNFα was induced in a dose-dependent manner. This was accompanied by reduced consumption of O_2 production of CO_2, reduced UCP1 expression in BAT and reduced insulin signal transduction through IRS1 and FOXO1 in the liver and muscle. Therefore, the icv treatment with stearic acid reproduces the effects of TNFα on peripheral parameters, reflecting thermogenesis and insulin action. In this context, recent data have shown that nutrients, including fatty acids, can activate hypothalamic S6 kinase, leading to hepatic resistance to insulin action (34).

A recent study has shown that the knockout of the main TNFα receptor, TNFR1, protects against DIO by an increased thermogenesis (7). We tested the hypothesis that the ability of low-grade hypothalamic inflammation to modulate peripheral insulin action may be intermediated by this receptor isotype. For this, TNFR1-KO mice were fed on a HF diet and evaluated for insulin signal transduction in the liver and muscle. Indeed, insulin responsiveness was completely preserved in KO mice compared with their controls, strongly suggesting that most the action of TNFα in the hypothalamus was delivered by this receptor. Because the KO mice employed were devoid of TNFR1 in the whole body, we designed an experiment to evaluate the specific action of TNFα in the hypothalamus; for this, HF diet-fed rats were treated icv with the anti-TNFα-neutralizing

antibody, infliximab, and thermogenesis and insulin signaling in peripheral tissues were evaluated. As expected, the hypothalamic immunoneutralization of TNFα in HF diet-fed rats completely restored defective thermogenesis and insulin signal transduction in liver and muscle.

We conclude that, in animal models of obesity, a low-grade hypothalamic inflammation takes place. This inflammatory response plays an important role in the local induction of resistance to leptin and insulin, which provides the neuroendocrine basis for the development of obesity. An important advance was obtained by linking hypothalamic inflammation with a defective insulin action and an effective thermogenesis in peripheral tissues. In addition, the adverse modulation of insulin secretion was observed. Although we have not explored the mechanisms that effectively deliver the neural signal to the affected peripheral organs, it is tempting to propose that the modulation of the sympathetic tonus could be involved. This work adds information to support a seminal role played by hypothalamic dysfunction in the genesis of glucose intolerance and DM2.

Acknowledgments

We thank Dr. N. Conran, from the University of Campinas, for English grammar edition and Mr. M. Cruz, from the University of Campinas for technical assistance.

Address all correspondence and requests for reprints to: Lício A. Velloso, Department of Internal Medicine, Faculty of Medical Sciences, University of Campinas, 13084-761 Campinas-Sao Paulo, Brazil. E-mail: lavelloso.unicamp@gmail.com.

This work was supported by Fundação de Amparo à Pesquisa do Estado de São Paulo and Conselho Nacional de Desenvolvimento Científico e Tecnológico. The Laboratory of Cell Signaling belongs to the Instituto Nacional de Ciência e Tecnologia-Obesidade e Metabolismo.

Disclosure Summary: The authors have nothing to declare.

References

1. **Hotamisligil GS** 2006 Inflammation and metabolic disorders. Nature 444:860–867
2. **Hotamisligil GS** 2010 Endoplasmic reticulum stress and the inflammatory basis of metabolic disease. Cell 140:900–917
3. **De Souza CT, Araujo EP, Bordin S, Ashimine R, Zollner RL, Boschero AC, Saad MJ, Velloso LA** 2005 Consumption of a fat-rich diet activates a proinflammatory response and induces insulin resistance in the hypothalamus. Endocrinology 146:4192–4199
4. **Milanski M, Degasperi G, Coope A, Morari J, Denis R, Cintra DE, Tsukumo DM, Anhe G, Amaral ME, Takahashi HK, Curi R, Oliveira HC, Carvalheira JB, Bordin S, Saad MJ, Velloso LA** 2009 Saturated fatty acids produce an inflammatory response predominantly through the activation of TLR4 signaling in hypothalamus: implications for the pathogenesis of obesity. J Neurosci 29:359–370
5. **Prada PO, Zecchin HG, Gasparetti AL, Torsoni MA, Ueno M, Hirata AE, Corezola do Amaral ME, Höer NF, Boschero AC, Saad MJ** 2005 Western diet modulates insulin signaling, c-Jun N-terminal kinase activity, and insulin receptor substrate-1ser307 phosphorylation in a tissue-specific fashion. Endocrinology 146:1576–1587
6. **Zhang X, Zhang G, Zhang H, Karin M, Bai H, Cai D** 2008 Hypothalamic IKKβ/NF-κB and ER stress link overnutrition to energy imbalance and obesity. Cell 135:61–73
7. **Romanatto T, Roman EA, Arruda AP, Denis RG, Solon C, Milanski M, Moraes JC, Bonfleur ML, Degasperi GR, Picardi PK, Hirabara S, Boschero AC, Curi R, Velloso LA** 2009 Deletion of tumor necrosis factor-α receptor 1 (TNFR1) protects against diet-induced obesity by means of increased thermogenesis. J Biol Chem 284:36213–36222
8. **Romanatto T, Cesquini M, Amaral ME, Roman EA, Moraes JC, Torsoni MA, Cruz-Neto AP, Velloso LA** 2007 TNF-α acts in the hypothalamus inhibiting food intake and increasing the respiratory quotient–effects on leptin and insulin signaling pathways. Peptides 28:1050–1058
9. **Johnson AK, Epstein AN** 1975 The cerebral ventricles as the avenue for the dipsogenic action of intracranial angiotensin. Brain Res 86: 399–418
10. **Cintra DE, Pauli JR, Araújo EP, Moraes JC, de Souza CT, Milanski M, Morari J, Gambero A, Saad MJ, Velloso LA** 2008 Interleukin-10 is a protective factor against diet-induced insulin resistance in liver. J Hepatol 48:628–637
11. **Arruda AP, Milanski M, Romanatto T, Solon C, Coope A, Alberici LC, Festuccia WT, Hirabara SM, Ropelle E, Curi R, Carvalheira JB, Vercesi AE, Velloso LA** 2010 Hypothalamic actions of tumor necrosis factor α provide the thermogenic core for the wastage syndrome in cachexia. Endocrinology 151:683–694
12. **Ropelle ER, Pauli JR, Zecchin KG, Ueno M, de Souza CT, Morari J, Faria MC, Velloso LA, Saad MJ, Carvalheira JB** 2007 A central role for neuronal adenosine 5′-monophosphate-activated protein kinase in cancer-induced anorexia. Endocrinology 148:5220–5229
13. **Maness LM, Kastin AJ, Farrell CL, Banks WA** 1998 Fate of leptin after intracerebroventricular injection into the mouse brain. Endocrinology 139:4556–4562
14. **Araújo EP, De Souza CT, Ueno M, Cintra DE, Bertolo MB, Carvalheira JB, Saad MJ, Velloso LA** 2007 Infliximab restores glucose homeostasis in an animal model of diet-induced obesity and diabetes. Endocrinology 148:5991–5997
15. **Bertelli DF, Araujo EP, Cesquini M, Stoppa GR, Gasparotto-Contessotto M, Toyama MH, Felix JV, Carvalheira JB, Michelini LC, Chiavegatto S, Boschero AC, Saad MJ, Lopes-Cendes I, Velloso LA** 2006 Phosphoinositide-specific inositol polyphosphate 5-phosphatase IV inhibits inositide trisphosphate accumulation in hypothalamus and regulates food intake and body weight. Endocrinology 147:5385–5399
16. **Scott AM, Atwater I, Rojas E** 1981 A method for the simultaneous measurement of insulin release and B cell membrane potential in single mouse islets of Langerhans. Diabetologia 21:470–475
17. **Andersson A** 1978 Isolated mouse pancreatic islets in culture: effects of serum and different culture media on the insulin production of the islets. Diabetologia 14:397–404
18. **Thaler JP, Choi SJ, Schwartz MW, Wisse BE** 2010 Hypothalamic inflammation and energy homeostasis: resolving the paradox. Front Neuroendocrinol 31:79–84
19. **Silva JE** 2006 Thermogenic mechanisms and their hormonal regulation. Physiol Rev 86:435–464
20. **Cannon B, Nedergaard J** 2004 Brown adipose tissue: function and physiological significance. Physiol Rev 84:277–359
21. **Kleinridders A, Schenten D, Könner AC, Belgardt BF, Mauer J, Okamura T, Wunderlich FT, Medzhitov R, Brüning JC** 2009 MyD88 signaling in the CNS is required for development of fatty acid-induced leptin resistance and diet-induced obesity. Cell Metab 10:249–259
22. **Muoio DM, Newgard CB** 2008 Mechanisms of disease: molecular

and metabolic mechanisms of insulin resistance and β-cell failure in type 2 diabetes. Nat Rev Mol Cell Biol 9:193–205

23. **Marchetti P, Lupi R, Del Guerra S, Bugliani M, D'Aleo V, Occhipinti M, Boggi U, Marselli L, Masini M** 2009 Goals of treatment for type 2 diabetes: β-cell preservation for glycemic control. Diabetes Care 32(Suppl 2):S178–S183
24. **DeFronzo RA** 2010 Current issues in the treatment of type 2 diabetes. Overview of newer agents: where treatment is going. Am J Med 123:S38–S48
25. **Hotamisligil GS, Arner P, Caro JF, Atkinson RL, Spiegelman BM** 1995 Increased adipose tissue expression of tumor necrosis factor-α in human obesity and insulin resistance. J Clin Invest 95:2409–2415
26. **Kayacan O, Karnak D, Beder S, Güllü E, Tutkak H, Senler FC, Köksal D** 2006 Impact of TNF-α and IL-6 levels on development of cachexia in newly diagnosed NSCLC patients. Am J Clin Oncol 29:328–335
27. **De Souza CT, Araújo EP, Stoppiglia LF, Pauli JR, Ropelle E, Rocco SA, Marin RM, Franchini KG, Carvalheira JB, Saad MJ, Boschero AC, Carneiro EM, Velloso LA** 2007 Inhibition of UCP2 expression reverses diet-induced diabetes mellitus by effects on both insulin secretion and action. FASEB J 21:1153–1163
28. **Pomp D, Nehrenberg D, Estrada-Smith D** 2008 Complex genetics of obesity in mouse models. Annu Rev Nutr 28:331–345
29. **Cypess AM, Lehman S, Williams G, Tal I, Rodman D, Goldfine AB, Kuo FC, Palmer EL, Tseng YH, Doria A, Kolodny GM, Kahn CR** 2009 Identification and importance of brown adipose tissue in adult humans. N Engl J Med 360:1509–1517
30. **Porte Jr D, Kahn SE** 2001 β-Cell dysfunction and failure in type 2 diabetes: potential mechanisms. Diabetes 50(Suppl 1):S160–S163
31. **Biddinger SB, Kahn CR** 2006 From mice to men: insights into the insulin resistance syndromes. Annu Rev Physiol 68:123–158
32. **Taniguchi CM, Emanuelli B, Kahn CR** 2006 Critical nodes in signalling pathways: insights into insulin action. Nat Rev Mol Cell Biol 7:85–96
33. **Benoit SC, Kemp CJ, Elias CF, Abplanalp W, Herman JP, Migrenne S, Lefevre AL, Cruciani-Guglielmacci C, Magnan C, Yu F, Niswender K, Irani BG, Holland WL, Clegg DJ** 2009 Palmitic acid mediates hypothalamic insulin resistance by altering PKC-θ subcellular localization in rodents. J Clin Invest 119:2577–2589
34. **Ono H, Pocai A, Wang Y, Sakoda H, Asano T, Backer JM, Schwartz GJ, Rossetti L** 2008 Activation of hypothalamic S6 kinase mediates diet-induced hepatic insulin resistance in rats. J Clin Invest 118:2959–2968